V European Conference on Computational Fluid Dynamics
ECCOMAS CFD 2010
J. C. F. Pereira and A. Sequeira (Eds)
Lisbon, Portugal,14-17 June 2010

ASSESSMENT OF PERFORMANCE OF LOW REYNOLDS TURBULENCE MODELS IN PREDICTING NATURAL

M. Aksouh*†, A. Mataoui† N. Seghouani* and Z. Haddad ††

*Department of Astronomy and Astrophysics, Centre of Research of Astronomy Astrophysics and Geophysics CRAAG, Algiers, Algeria
Route de l'obseravtoire BP63 Bouzareah Algiers 16340 Algeria
e-mail: m.aksouh@craag.dz
†Theoretical and applied laboratory of fluid mechanics, University of science and Technology of Algiers USTHB, Algiers, Algeria
e-mail: mataoui_amina@yahoo.fr
††University of Boumerdes, Boumerdes, Algeria.

Key words: Natural turbulent convection, numerical simulation, low-Reynolds number, rectangular cavity, turbulence modeling

Abstract. *The three dimensional study of natural convection in enclosure cavities is receiving more and more research attention due to its interesting practical applications in the engineering domain. In this work, the turbulent natural convection of air in enclosed tall cavity with high aspect ratio (AR=height/width=28.6) is examined numerically. Two cases of differential temperature have been considered, 19.6 C and 39 C between two vertical lateral cavity plates, which correspond to low and high Rayleigh number respectively. The flow is extremely slow for the two cases of differential temperature except in the core cavity where it becomes turbulent. This led us to improve the flow in the rectangular cavity by using two low-Reynolds number turbulence models: RNG $k-\epsilon$ model and SST $k-\omega$ model, which are derived from standard $k-\epsilon$ model and standard $k-\omega$ model, respectively. Finally, in the order to check the suitable turbulence model for this kind of flow, the numerical results are compared with previous experimental data. A good agreement has been obtained between the numerical results and experiment.*

1 INTRODUCTION

The turbulent convection flows are omnipresent in the several sciences domain (Solar and stellar structure, Earth mantle, atmospheric turbulence, engineering, electronics). The turbulent convection flow depends directly on the fluid physiochemical properties and the geometric conditions. Usually, the natural convection flow, laminar or turbulent, is characterized by the Rayleigh number, which is defined by the following expression:

$$Ra = \frac{g\beta\delta TW}{a\nu}$$

This work, is carried out numerically to improve the structure of natural turbulence convection flows in an enclosure with high aspect ratio. For this process of heat transfer, theoretical, experimental and numerically studies have been performed. The numerical study of the enclosure turbulent natural convection becomes more complicated when the configuration is three-dimensional and the Reynolds number is low. In fact, this paper is the further of our work done previously [1], which consisted to study numerically the turbulent natural convection of air in the tall cavity by using two turbulence models: the standard $k-\epsilon$ model and its derivative RNG $k-\epsilon$ model. The comparison between the numerical results and the experimental data of Betts and Bokhari [4] showed that the results were very satisfactory for the RNG model compared to its standard model. However, the principal aim of this work is to study the same problem by using two turbulence low-Re models number: RNG $k-\epsilon$ model [19] and SST $k-\omega$ model [11]. The experiment of Betts and Bokhari [4] concerns the natural convection of air in an enclosed tall differentially heated rectangular cavity: $0.076m \times 2.18m \times 0.52m$ (corresponding to the width 'W', height 'H' and depth 'D' of cavity, respectively). The ratio between the height and width corresponds to a aspect ratio cavity (AR=H/W=28.6). The natural convection flow is generated by two differential temperatures between the two vertical lateral plates 19.6C and 39.9C. Under theses physical and geometries conditions, the flow in the core of the cavity is fully turbulent with low Reynolds number [4] and the temperature in the core becomes stratified [7]. However, the expression of Reynolds number is:

$$Re = \frac{UW}{\nu}$$

The numerical results for the vertical velocity, the temperature and the turbulent kinetic energy are compared to the experiment data. Also, the numerical results of the average Nusselt number along the hot vertical plate are compared to the experiment value of Betts and Bokhari [4] and the numerical results of Heish and Lien [8]. However, after the choice of turbulence model, the second objective of this work is to predict the variation of the wall heat transfer for various value of Rayleigh number. The theoretical study and experimental measurements [3,7,18,20] acquire a correlation between the average Nusselt number and Rayleigh number as follow: $N_u = C.Ra^m$, with the exponent, $m \approx 1/3$.

2 TURBULENCE MODELS

The steady turbulent compressible flow for the natural convection is studied through the steady Reynolds average Navies-Stokes equations coupled to the average energy equation [1–22]. These equations contain respectively the Reynolds stress terms and other correlations of the fluctuating velocity and scalar for which require a closure. The Reynolds stresses appearing in the Reynolds equations have been modeled by using two one point closure turbulence models recommended for low Re number: RNG $k-\epsilon$ model and SST $k-\omega$ model.

2.1 RNG $k-\epsilon$ model

The Renormalization group (RNG) methods are essential in near wall turbulence modeling for the asymptotic properties of their scales (the space and time fluctuations exist over all scales). On the basis of the scale invariance, inherent characteristic of the critical phenomena, the method allows to obtain systematically the intrinsic properties of the system constituents. Yakhot and Orszag in 1986 [19] derived from the standard $k-\epsilon$ model the RNG $k-\epsilon$ model by using The Renormalisation group (RNG) methods. The form of RNG model is summarized as follow:

$$\frac{\partial\left(\rho k u_i\right)}{\partial x_i}=\frac{\partial}{\partial x_j}\left[\alpha_k \mu_{eff}\frac{\partial k}{\partial x_j}\right]-\rho\epsilon+R_{ij}\frac{\partial u_i}{\partial x_j}+G_k \tag{1}$$

$$\frac{\partial\left(\rho\epsilon u_i\right)}{\partial x_i}=\frac{\partial}{\partial x_j}\left[\alpha_\epsilon \mu_{eff}\frac{\partial \epsilon}{\partial x_j}\right]+C_{\epsilon 1RNG}\frac{\epsilon}{\kappa}\left(R_{ij}\frac{\partial u_i}{\partial x_j}+G_k\right)-C^*_{\epsilon 2}\rho\frac{\epsilon^2}{k} \tag{2}$$

Where: $C^*_{\epsilon 2}=C_{\epsilon 2RNG}+\dfrac{C_{\mu RNG}\eta^3\left(1-\eta/\eta_0\right)}{1+\alpha\eta}$ and $\eta=\sqrt{2\left|D(u)\right|^2}\dfrac{k}{\epsilon}$

α_k and α_ϵ are the inverse Prandtl numbers for k and ϵ, respectively; and $C_{\epsilon 1RNG}=1.44$, $C_{\epsilon 2RNG}=1.92$, $C_{\mu RNG}=0.0845$, $\eta_0=4.38$ and $\alpha=0.012$.

$D(u)=\frac{1}{2}(\nabla u+\nabla^t u)$ is the mean strain rate tensor.

The difference between the RNG model and standard model is significant for flows within the large strain rates ($\eta<\eta_0$), where the additional term in equation becomes significant. In the limit of weak strain the supplementary source term tends to zero and the original form of the standard model is then recovered. The effective viscosity is calculated by a differential equation:

$$d\left(\frac{\rho^2 k}{\sqrt{\epsilon\mu}}\right)=1.72\frac{\widehat{\mu}}{\sqrt{\widehat{\mu}^3-1+C_{\widehat{\mu}}}}d\widehat{\mu} \tag{3}$$

where $\widehat{\mu}=\mu_{eff}/\mu$ and $C_{\widehat{\mu}}\approx=100$

2.2 SST $k-\omega$ model

In 1993, Menter [11] developed a new turbulence model based on the shear stress transport $k-\omega$ model. The principle of the SST method is to use the $k-\omega$ formulation in the inner zone of the boundary layer and the free-stream independence of the $k-\epsilon$ model in the outer part of the boundary layer. To combine these two models together, the standard $k-\epsilon$ model has been transformed into equations based on k and ω, which leads to the introduction of a cross-diffusion term in dissipation rate equation. The formalism of SST model is:

$$\frac{D\rho k}{Dt} = \tau_{ij}\frac{\partial u_i}{\partial x_j} - \beta^*\rho\omega k + \frac{\partial}{\partial x_j}\left[\left(\mu + \sigma_k\mu_t\right)\frac{\partial k}{\partial x_j}\right] \tag{4}$$

$$\frac{D\rho\omega}{Dt} = \frac{\gamma}{\nu_t}\tau_{ij}\frac{\partial u_i}{\partial x_j} - \beta\rho\omega^2 + \frac{\partial}{\partial x_j}\left[\left(\mu + \sigma_\omega\mu_t\right)\frac{\partial \omega}{\partial x_j}\right] + 2\left(1-F_1\right)\rho\sigma_{\omega 2}\frac{1}{\omega}\frac{\partial k}{\partial x_j}\frac{\partial \omega}{\partial x_j} \tag{5}$$

The difference between the SST formulation and the original $k-\omega$ model is that an additional cross-diffusion terms appears in the ω equation and the modeling constants ϕ are different with the following relation :

$$\phi = F\phi_1 + (1-F)\,\phi_2 \tag{6}$$

ϕ_1 and ϕ_2 represent any constant in the original $k-\omega$ model and in the transformed $k-\epsilon$ model, respectively.

where:

$$F = \tanh\left(\Lambda^2\right) \tag{7}$$

and

$$\Lambda = \max\left(2\frac{\sqrt{k}}{0.09\omega y}; \frac{500\nu}{y^2\omega}\right) \tag{8}$$

3 NUMERICAL PROCEDURE

We consider a tall rectangular cavity for air with high aspect ratio AR=H/W=28.68, the dimensions of cavity are: $0.076 \times 2.18 \times 0.52(m)$, as showing in the figure 1. The spatial derivatives in the equations are discretized with the finite volume method which requires refined meshes near the wall (Pantankar [14]). The principle of the finite volume method is that the governing equations can be reformulated under the general equations as follows:

$$\left(\rho u_i\Phi\right)_{,i} = \left(\Gamma\frac{\partial\Phi}{\partial x_i}\right)_{,i} \tag{9}$$

and this general equation is converted into the algebraic equation with the following form:

$$a_P \phi_P^{n+1} = \sum_{nb} a_{nb} \phi_{nb}^{n+1} + S_\phi \Delta V + \rho^n \Delta V \phi_P^n \tag{10}$$

where n is the iteration number and nb is specification of the neighbor grids (representing north, east, south, west point).
Since the flow is steady in average, the SIMPLE algorithm is applied for the pressure-velocity coupling and the power law scheme is use for the interpolation process. Using the low-Reynolds number turbulence models require refined grid in the inner zone of the boundary layer. Different grids sizes are tested previously [1]. The present numerical results in this work are achieved by $50 \times 300 \times 50$ rectangular non-uniform cells. For the boundary conditions, two differential temperatures are applied between the lateral plates $19.6C$ and $39.9C$, as showing in table 1. The front, back, bottom and top walls were kept adiabatic with no slip condition, U=0.

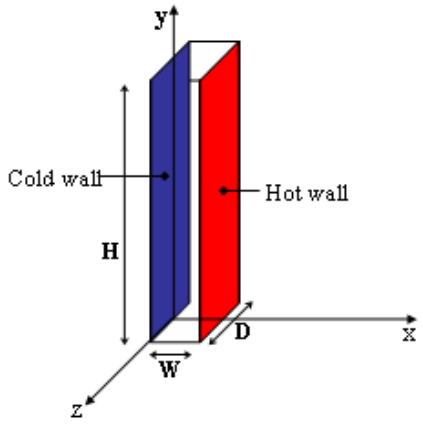

Figure 1: The geometry of the configuration

	Cold wall	Hot wall	Ra
First case	15.1C	34.7C	0.86×10^6
Second case	15.6C	55.5C	1.43×10^6

Table 1: Examined conditions

4 RESULTS AND DISCUSSION

4.1 The vertical velocity

At hight position (for y/H=0.5, z=0), the numerical results and the experimental data [4] for the mean vertical velocity are plotted in the figures 2.a and 2.b, corresponding to the

low and high Rayleigh number respectively. The distribution of the vertical velocity indicates that the velocity gradient is more important near the wall, and the profile have two peaks which reveal that the fluid particles heated near the hot walls are moved upward along the hot wall and the cold fluid particles are pulled downward along the cold wall. In the core region (y/H=0.5, x/W=0.5, z=0) the flow is practically quiescent ($vy \approx 0$), i.e. the air is almost stagnant at the center of cavity [3].
The profiles for both turbulence models , RNG and SST models, are in good agreement with experimental data and the predictions difference is minor. However, for more precision, the table 2 represents the maximum of the mean vertical velocity for the two models, which are compared to the experimental data. The error between the two models and the experimental data are indicated in brackets, where:

$$Er = \left(R_{exp} - R_{num}\right)/R_{exp} \tag{11}$$

It should be noted that the vertical velocity peak determined by SST $k-\omega$ model is better than RNG $k-\epsilon$ model. This reveals the importance of the SST $k-\omega$ model for low Reynolds number case where the gradient is more important near the wall. Furthermore , near the wall is viscous boundary layer in where the velocity increases with distance from the wall and where the velocity gradient is strongest. Also, near the wall the vorticity is large. Thus, the vorticity, which represent the rate of spin of particle fluid, is defined as the curl of velocity (equation 12). In this study, the configuration is three dimension, thus each point in the fluid has an associated vector vorticity in three dimensions. However, the temperature and flow field were founded to be closely two-dimensional [4], so the vorticity vector is normal to the plan (x,y). The figure 3 represents the vorticity components for the three direction at different height, it is is clearly evident that flow is two dimension with normal vorticity in the z direction. The figure shows that the normal vorticity magnitude is maximum near the wall where maximal velocity occur. However, the high vorticity near wall region originates from shear stress and not from a swirling or rotational motion [22]. The contours of the normal vorticity, plotted in the figures 4, show that near the cold surface the vorticity is concentrated into the down flow at the top of cavity and in the other side it is concentrated near the hot wall at the bottom of cavity.In addition, the vorticity magnitude increase with Rayleigh number.

$$\omega = \nabla \times \mathbf{U} \tag{12}$$

	$\overline{\nu_y}$ $(LowRa)$	$\overline{\nu_y}$ $(HighRa)$
Experiment (Betts and Bokhari, 2000)	0.14	0.19
Numerical results for RNG model	0.170328(17.81%)	0.240864(21.12%)
Numerical results for SST model	0.13197(5.8%)	0.23022(17.48%)

Table 2: The maximum vertical velocity for different methods, $(y/H = 0.5, z = 0)$

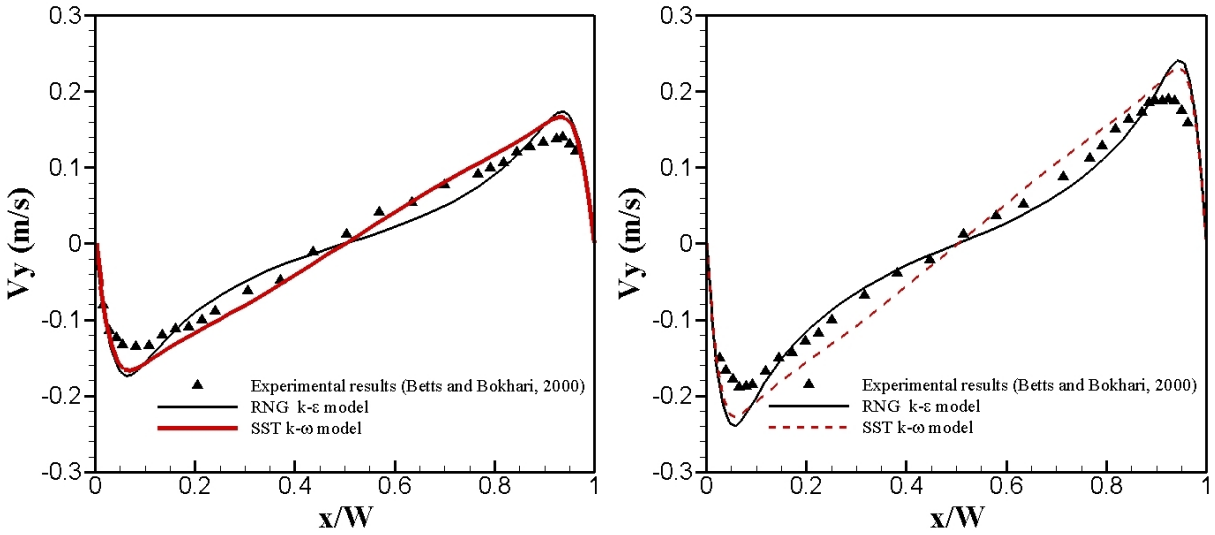

(a) Low Ra (b) High Ra

Figure 2: The vertical velocity profile across the cavity width at mid-height ($X = 0.5$, $Y = 0.5 and Z = 0$)

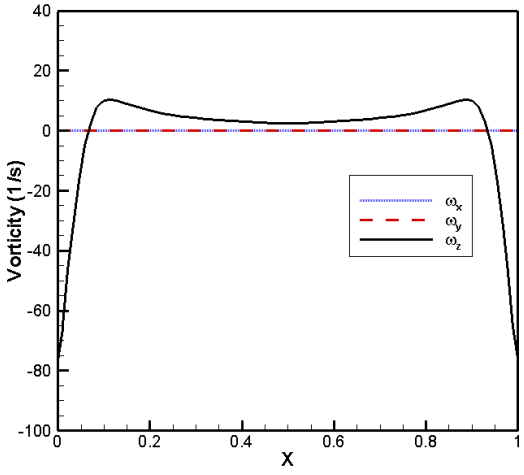

Figure 3: The profile of the vorticity axis at mid-height ($X = 0.5$, $Y = 0.5\, and\, Z = 0$)

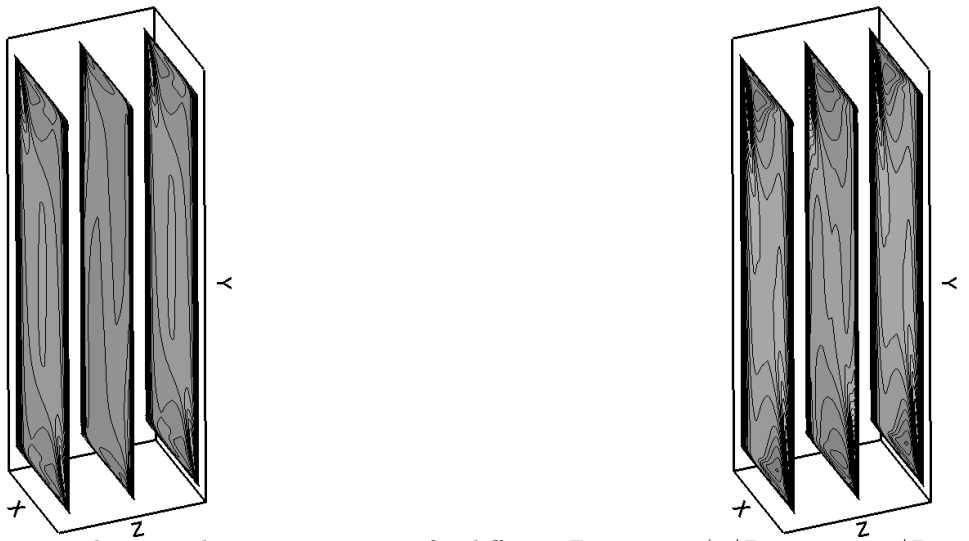

Figure 4: The normal vorticity contours for different Z positions ($z/D = -0.25$, $z/D = 0 and z/D = 0.25$)

4.2 The temperature profiles

The mean temperatures profiles for low and high Rayleigh numbers are plotted in the figure 5.a and figure 5.b, respectively, from the cold wall to the hot wall at cavity mid height (y/H=0.5). The numerical results are in good harmony with experimental data for the SST $k-\omega$ model and RNG $k-\epsilon$ model. Similar to the mean vertical velocity evolution, the mean temperature shows high gradients near the wall boundary layer with a somewhat linear variation in the cavity core. Xaman et al. [18] explain this result that in addition to the heat transported by natural convection along the surface of both hot and cold walls, there is heat conduction through the central core of the layer. Also, the temperature profiles are linear near the wall which represent the conductive and viscous sublayers.

4.3 The turbulent kinetic energy

To compare the different results for the turbulent kinetic energy we use the equation 13 to calculate k for the experimental data, since the data do not provide the results for $\acute{w}$ and is it very difficult to estimate $\acute{w}$ for the anisotropic turbulent natural convection without direct measurement.

$$k_{exp} = \frac{1.5\left(\overline{\acute{u}^2} + \overline{\acute{v}^2}\right)}{2} \tag{13}$$

The figures 6.a and 6.b illustrate the profiles of the turbulent kinetic energy at mid height of the tall cavity. For the fluctuating values, the both models produce reasonably numerical results for the turbulent kinetic energy compared to experimental data. In the center of the cavity (x/W=0.5) the turbulent kinetic energy is high inversely to the vertical

velocity which is practically zero, this zone is considered as the the outer layer. The figures show clearly that the level of turbulent kinetic energy increase with Rayleigh number.

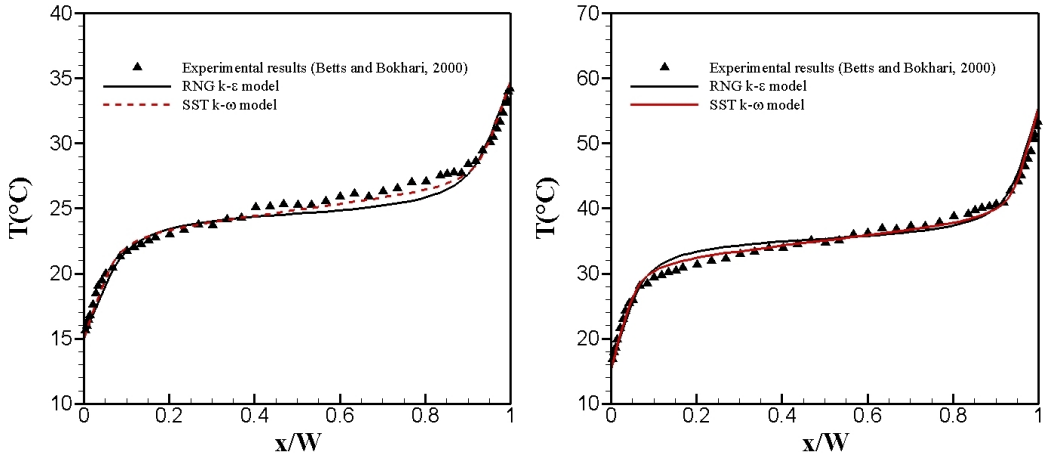

(a) Low Ra (b) High Ra

Figure 5: The temperature profile across the cavity width at mid-height ($X = 0.5$, $Y = 0.5$ *and* $Z = 0$)

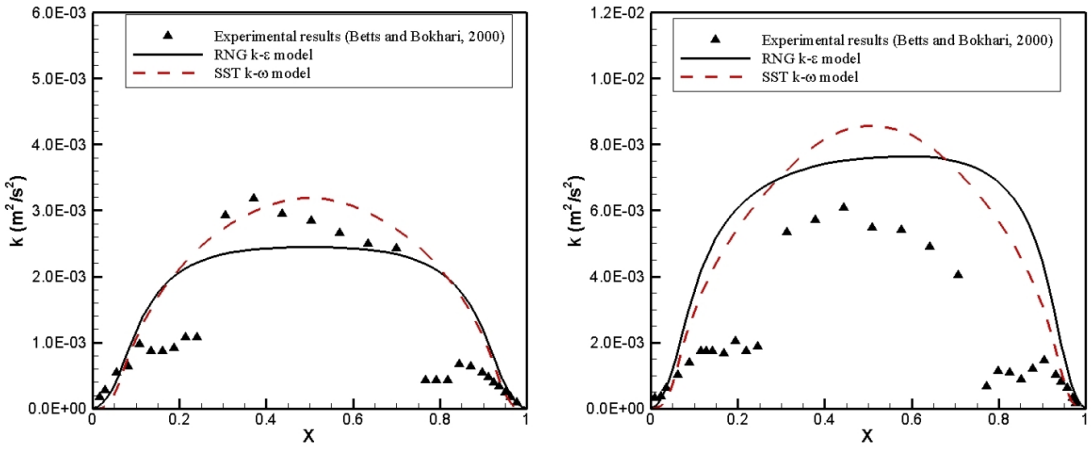

(a) Low Ra (b) High Ra

Figure 6: The turbulent kinetic energy profile across the cavity width at mid-height ($X = 0.5$, $Y = 0.5$ *and* $Z = 0$)

4.4 Heat transfer

The heat transfer of fluid along the heated wall is defined by dimensionless number, which characterizes the ratio of convective to conductive heat transfer across the boundary. The dimensionless number is the Nusselt number:

$$Nu = -\frac{L}{T_h - T_c}\frac{\partial T}{\partial n} \tag{14}$$

The average Nusselt number along the heated vertical wall is deduced from the last equation:

$$\overline{Nu} = -\frac{\int_0^H Nu\ dy}{H} \tag{15}$$

The different value of the average Nusselt number along the hot wall for the both models (SST and RNG models), experimental value [4] and the numerical results for Hsieh and Lien [8] are referred in the table 3. Heish and Lien [8] used the unsteady RANS approach combined with low-Re $k-\epsilon$ model of Lien and Leschnizer[9] to simulate the flow in the tall cavity by considering the flow in 2D. They founded that the steady RANS can be used to compute this flow without meeting convergence problems. The results in the table 3 show that the better predictions are obtained by the SST $k-\omega$ model, especially for low Rayleigh number cases. But the difference is not important compared to the RNG $k-\epsilon$ model. Usually, the heat transfer depends on the Rayleigh number, Prandtl number and the aspect ratio as: Nu=f(Ra, Pr, AR). In this work, Prandtl number (Pr) does not vary significantly within the range of the considered temperature, and the dimensions of the cavity are. So, we have just to examine the variation of the average Nusselt number versus the Rayleigh number.

	$\overline{Nu_y}$ $(LowRa)$	$\overline{Nu_y}$ $(HighRa)$
Numerical results (Hsieh and Lien [8])	–	6.39 (15.59%)
Experimental data(Betts and Bokhari [4])	5.85	7.57
Numerical results for RNG model	5.51 (5.81%))	6.905 (8.78%))
Numerical results for SST model	5.66 (3.25%))	6.96 (8.06%))

Table 3: Average Nusselt number near the hot wall for high and low Rayleigh number.

In order to correlate this variation, different differential temperatures between the two vertical plates have been applied (table 4) and only the SST $k-\omega$ model is considered to simulate different flows in this part. Nevertheless, MacGregor and Emery, Cowan et al.,

Henkes et al [7], Betts and Dafa'alla [6] measured the flow in the different cavities sizes, all gave an averaged wall-heat transfer correlation by a power law like the expression :

$$Nu = c.Ra^{1/3} \tag{16}$$

Where the constant c is somewhat different (c=0.046, 0.043, 0.047 and 0.053, respectively).

So, the figure 7 represents the variation of the Nusselt versus the Rayleigh number with logarithmic axis. According to the equation 16 and after fitting by a linear interpolation, we find that the c constant is 0.062. In this work, for the tall cavity with high aspect ratio (AR=28.68), the correlation between the Rayleigh number and the Nusselt number is proposed by the following relation:

$$Nu = 0.062.Ra^{1/3} \tag{17}$$

Ra	$\overline{Nu}$
$0.86E+6$	5.66
$0.95E+6$	6.54
$1.11E+6$	6.66
$1.25E+6$	6.92
$1.43E+6$	6.96

Table 4: Average Nusselt number by SST model for different Rayleigh number.

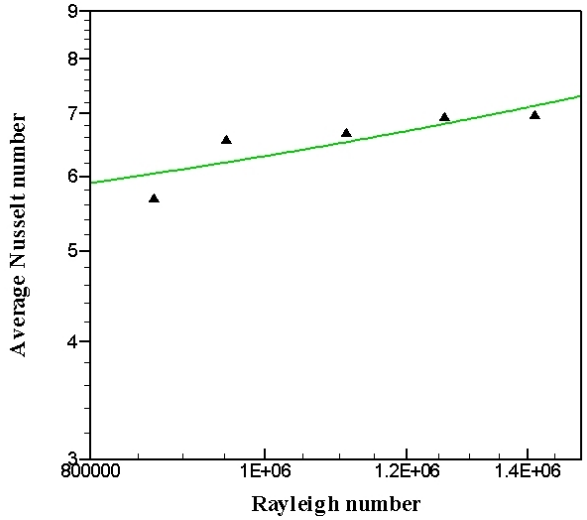

Figure 7: Profile of the average Nusselt number versus the Rayleigh number.

5 CONCLUSIONS

- In this work, a three dimensional numerical study has been investigated using two one point closure models: RNG $k-\epsilon$ model and SST $k-\omega$ model.
- The numerical results are compared to the experimental data obtained by Betts and Bokhari for the turbulent natural convection of air.
- A good agreement between the experiment and numerical prediction is observed for the RNG $k-\epsilon$ model and SST $k-\omega$ model. However, SST $k-\omega$ model is better near the walls and for the heat transfer.
- The profiles of the mean vertical velocity, mean temperature and the turbulent kinetic energy denote that the flow in the core region of the tall cavity is very weak and the turbulence level increases.
- Finally, for the different Rayleigh number, a correlation between the Rayleigh number and the Nusselt number is proposed.

REFERENCES

[1] M. Aksouh, A. Mataoui Numerical study of the turbulent natural convection in an enclosed tall cavity for the high and low Rayleigh number, *Advanced Computational Methods in Engineering*, ACOMEN 2008, Liege, Belgium

[2] F. Ampofo, T. G. Karayiannis, Experimental benchmark data for turbulent natural convection in an air filled square cavity, *Int. J. Heat Mass transfer*, **46**, 3551-3572 (2003).

[3] M. Aounallah et *al.* Numerical investigation of turbulent natural convection in an inclined square cavity with a hot wavy wall, *Intr. J. of Heat and Mass Transfer*, **50**, 1683-1693 (2007).

[4] P.L. Betts and I.H. Bokhari, Experiments on natural convection in an enclosed tall cavity, *Intr. J. of Heat and fluid flow*, **21**, 675-683 (2000).

[5] R. Cheesewright, K. J. King, S. Ziai, Experimental data for the validation of computer codes for the prediction of two-dimensional buoyant cavity flows, *ASME Winter Annual Meeting*, HTD 60, pp. 75-81, (1986).

[6] A.A. Dafa'Alla and P.L. Betts, Experimental study of turbulent natural convection in a tall air cavity, *Exp Heat Transfer*, **9**, 165-194 (1996).

[7] R. A. W. M. Henkes, F. F. Vander Flugt, C. J. Hoogendoorn, Natural Convection Flow in a Square Cavity Calculated with Low-Reynolds-Number Turbulence Models. *Int. J. Heat Mass Transfer*, **34**, 1543-1557 (1991).

[8] K. J. Hsieh, F. S. Lien, Numerical modeling of buoyancy-driven turbulent flows in enclosures, *International Journal of Heat and Fluid Flow*, **25**, 659-670 (2004).

[9] F. S. Lien, M. A. Leschziner, Computational modeling of a transitional 3D turbine-cascade flow using a modified low-Re $k-\epsilon model$ and a multi-block scheme, *International Journal of Computational Fluid Dynamics*, **12**, 1-15 (1999).

[10] K. Matsusaki, H. OHBA, M. Munekata, Numerical analysis of thermal convections in a three dimensional cavity: Influence of difference in approximation models on numerical solutions, *J. of Thermal science*, **13**, 283-288(2003).

[11] F. R. Menter, Two-Equation Eddy-Viscosity Turbulence Models for Engineering Applications, *AIAA Journal*, **32(8)**, 1598-1605 (1994).

[12] S. Mergui, F. Penot, Convection naturelle en cavit carre diffrentiellement chauffe : investigation exprimentale $Ra = 1.69 \times 10^9$, *International Journal of Heat and Mass Transfer*, Vol. **39**, 563-574, (1996).

[13] M. Ouriemi, P. Vasseur, A. Bahloul, Natural convection of a binary mixture confined in a slightly inclined tall enclosure, *Int. C. Heat mass transfer*, **32**, 770-778 (2005).

[14] S. V. Patankar, Numerical heat transfer and fluid flow, Series in Computational methods in mechanics and thermal sciences, *Mc Graw Hill*, Hemisphere Publishing Corp, (1981).

[15] Y. S. Tian, T. G. Karayiannis, Low turbulence natural convection in an air filled square cavity. Part I: the thermal and fluid flow fields, *International Journal of Heat and Mass Transfer*, **43**, 849-866 (2000).

[16] W. Vieser, T. Esch, F. Menter, Heat transfer predictions using advanced two-equation turbulence models, *CFX Validation Report*, **CFX-VAL10/0902**, (2002).

[17] D. C. Wilcox, Turbulence Modeling for CFD, *DCW Industries Inc*, La Canada, CA, (1994).

[18] J. Xaman, G.Alvarez, L. Lira, C. Estrada, Numerical study of heat transfer by laminar and turbulent natural convection in tall cavities of faade elements. *Energy and Buildings*, **37**, 787-794 (2005).

[19] V. Yakhot, S. A. Orszag, Renormalization Group Analysis of turbulence. *Journal of scientific Computing*, **1**, 3-51 (1986).

[20] H. Yang, Z. Zhu, Numerical study of three-dimensional turbulent natural convection in a differentially heated air-filled tall cavity, *Int. C. Heat and Mass Transfer*, **35**, 606-612 (2008).

[21] O. Younis, J. Pallares, F. X. Grau, Numerical study of transient laminar natural convection cooling of high Prandtl number fluids in cubical cavity: Influence of the Prandtl number, *IJSET*, **4**, 1307-4318 (2007).

[22] S. Kenjeres, K. Hanjalic,Transient analysis of Rayleigh-Benard convection with a RANS model, *International Journal of Heat and Fluid Flow*, **20**, 329-340 (1999).